Research Article

Jiang Zhao, Shuangyuan Wang, Qiufan Wang*, and Daohong Zhang*

Closed-loop recycling and fabrication of hydrophilic CNT films with high performance

https://doi.org/10.1515/ntrev-2022-0075
received October 23, 2021; accepted March 17, 2022

Abstract: Carbon nanotube (CNT) film has attracted tremendous attention in functional material research for its unique structure and excellent properties. However, pristine CNT (PCNT) film is hydrophobic, and mechanical strength and conductivity are poor than reported individual CNT. These challenges impede its wide application. Highly efficient closed-loop recycling of both monomer and CNT film is a major challenge. Herein, hydrophilic CNT film with high mechanical strength and conductivity was prepared under the synergistic effects of *in situ* nitrogen doping and thiol-ene click reaction. The tensile strength, Young's modulus, and electrical conductivity both in perpendicular and in longitudinal directions are 1,362, 1,658, 222, and 218% higher than those of PCNT film. Closed-loop recycling of CNT film and monomer with high recyclability (100 and 86.72%) has been achieved in a gentle acid environment. The CNT films are 100% recovered and reused to fabricate thiol-functionalized CNT film without deterioration of performance after three cycles, which provides a novel strategy for the preparation of high-performance CNT film and a pathway for high-efficiency closed-loop recycling of CNT film and monomer.

Keywords: carbon nanotube film, *in situ* nitrogen doping, thiol-ene click reaction, hydrophilic, high performance, closed-loop recycling

*** Corresponding author: Qiufan Wang,** Key Laboratory of Catalysis and Energy Materials Chemistry of Ministry of Education & Hubei Key Laboratory of Catalysis and Materials Science, Hubei R&D Center of Hyperbranched Polymers Synthesis and Applications, South-Central University for Nationalities, Wuhan 430074, China, e-mail: ygdf@mail.scuec.edu.cn

*** Corresponding author: Daohong Zhang,** Key Laboratory of Catalysis and Energy Materials Chemistry of Ministry of Education & Hubei Key Laboratory of Catalysis and Materials Science, Hubei R&D Center of Hyperbranched Polymers Synthesis and Applications, South-Central University for Nationalities, Wuhan 430074, China, e-mail: daohong.zhang@scuec.edu.cn, zhangdh27@163.com

Jiang Zhao, Shuangyuan Wang: Key Laboratory of Catalysis and Energy Materials Chemistry of Ministry of Education & Hubei Key Laboratory of Catalysis and Materials Science, Hubei R&D Center of Hyperbranched Polymers Synthesis and Applications, South-Central University for Nationalities, Wuhan 430074, China

1 Introduction

Since carbon nanotubes (CNTs) were first reported in 1991 [1], it has undergone three decades of vigorous development. CNT has increasingly attracted enormous attention from researchers in both academic and industry and is widely applied in energy applications [2,3], artificial muscles [4], sensors [5], catalytic materials [6], separation and purification [7], electromagnetic interference shielding [8], and aerospace [9] as a consequence of its high specific surface area, extraordinary lightweight, high mechanical strength, biocompatibility, and electrical, thermal, optical properties [10]. But pristine CNT (PCNT) films are hydrophobic and inert [11], which leads to poor compatibility with other materials and restricts their application in an aqueous environment. Simultaneously, due to the low interfacial interaction and orientation, PCNT films possess lower conductivity and mechanical performance [12]. Modification of CNT films as an approach to overcome these shortcomings mentioned above is of great significance.

The strategies to modify CNT films are generally divided into physical and chemical methods. Physical methods mainly include hot-pressing densification [13], mechanical rolling [14], dipping of organic solvents [15], polymer infiltration [16], physical doping [17], heat treatment [18], and electric treatment [19]. Physical methods may bring out many disadvantages. For instance, pressing and rolling lead to the collapse phenomenon, which enlarges the interface surface area between CNTs and destroys the overall mechanical performance of the bundles [20]. The main challenge of polymer infiltration of CNT networks is composites with heterogeneous morphologies and poor mechanical properties as a consequence of stress concentrations at voids within the composite. On the contrary, chemical modification is usually to form a covalent bond between CNTs or surface modification with some chemical

groups to promote tensile strength, conductivity, and hydrophilicity.

Chemical methods can introduce various atoms, such as nitrogen, oxygen, phosphorus, sulfur, and so on [21–23]. It has been revealed that nitrogen-doped carbon nanostructures are promising to produce functional materials for various applications [24,25]. Nitrogen atoms can increase the specific surface area of CNTs, the contact site of electrolyte and electrode materials, and improve wettability [26]. Nitrogen atoms can enhance charge transfer to improve electric conductivity and increase load transfer to improve mechanical strength [21]. Nitrogen doping is divided into *in situ* nitrogen doping and post-treatment nitrogen doping. The difference between *in situ* nitrogen doping and traditional chemical vapor deposition (CVD) method is the utilization of nitrogen sources. Therefore, *in situ* nitrogen doping is a simple and commonly used approach. *In situ* nitrogen doping is conducive to changing the structure of CNTs, accelerating charge transfer, and enhancing conductivity [27]. But the effect of increasing the interaction between tubes is limited. Post-treatment nitrogen doping mainly includes the input of chemical group, convent bond, and noncovalent bond such as hydrogen bond. Post-treatment nitrogen doping is a more effective approach to improve wettability and mechanical strength. But the reported research studies about nitrogen doping are complicated and non-degradable. The extensive use of CNTs and CNT-based electrical waste brings out a great threat to human health and living environment [28].

Herein, two kinds of hydrophilic CNT films are fabricated by the CVD method using ferrocene as a catalyst, thiophene as a co-catalyst, ethanol and acetone as carbon sources, and melamine or ammonia bicarbonate as nitrogen sources, respectively. Two CNT films are respectively named NC-1 (ammonium bicarbonate as nitrogen source) and NC-2 (melamine as nitrogen source). Moreover, we chose three mercaptans with excellent wettability on PCNT film to prepare three hydrophilic CNT films by thiol-ene click reaction (Figure S2), one of the most utilized click reactions in materials science [29]. The three mercaptans are aminoethanethiol hydrochloride (AH), 2,2′,2″-(1,3,5-hexahydro-*s*-triazine-1,3,5-triyl) ethyl mercaptan (HT-EM), and 2,2′,2″-(1,3,5-hexahydro-*s*-triazine-1,3,5-triyl) benzyl mercaptan (HT-BM). Three CNT films modified by AH, HT-EM, and HT-BM are named AC, EC, and HC, respectively. Then, HNC-2 with higher mechanical strength (332 MPa) and electrical conductivity (675 S/cm) was prepared using the synergistic effects of the two methods. Interestingly, the wettability of CNT films is converted from hydrophobic to hydrophilic, which is beneficial to expand the application of CNT films. At the same time, the tensile strength, modulus, and electrical conductivity of functionalized CNT films were improved. But just tuning the wettability of CNT film from hydrophilic to hydrophobic is not enough to satisfy the need for various and different wettability. In order to deal with this problem, we prepared functionalized CNT film with controllable wettability by adjusting the amount of 2,2′,2″-(1,3,5-Hexahydro-*s*-triazine-1,3,5-triyl) benzyl mercaptan (HT-BM). More significantly, the design of recyclable hexahydro-s-triazine made functionalized CNT film degradable. And our research achieved closed-loop recycling of CNT films, a monomer with high recyclability (100 and 86.72%) as shown in Figure 1. And the degradation and cycle mechanism of resignation was researched. Although the tensile strength and electrical conductivity of recovered CNT film after three times close-loop recycling and the monomer of mercaptan have not been completely recycled, 100% of CNT film has been reused to prepare functionalized CNT film with no obvious performance degradation and over 80% of the monomer is recycled and reused to prepare mercaptan. Closed-loop recycling of CNT film and the monomer is significant in saving resources and protecting the environment in the field of nanotechnology to overcome abundant waste and the cost of materials. The consumption of CNT films is increasing year by year. CNTs do harm to human health and the environment, but a lot of CNT films have hardly been treated or recycled after use. In recent years, closed-loop

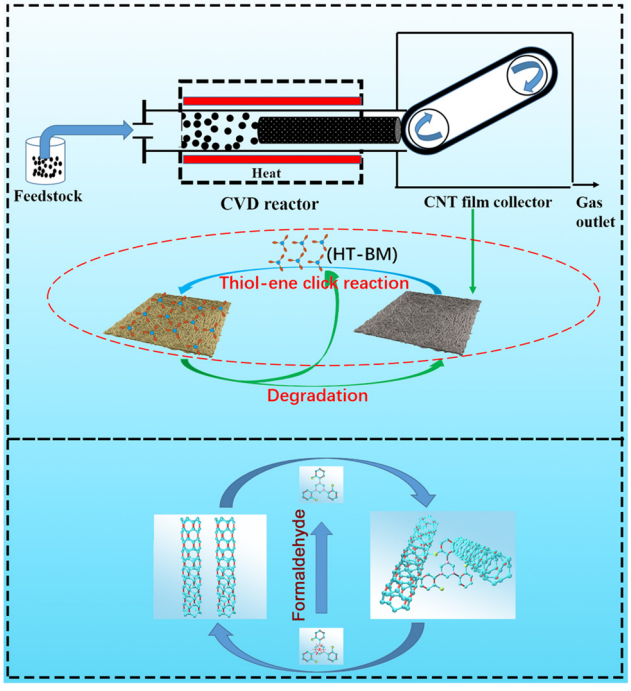

Figure 1: Closed-loop process thiol-functionalized CNT film for recycling both CNT film and monomer.

recycling of carbon fiber composites and recycling of CNT films have provided an efficient and popular method for the recycling of carbon nanometer materials [30–34]. And recent mechanism studies of recyclable hexahydro-s-triazine provide significant theoretical support [35–37]. Thus, closed-loop recycling of CNT film and monomer is realized successfully and the degradation and recycling mechanism has been proposed, which will be furtherly promising to apply in CNT-film-based batteries and supercapacitors. This material will be able to be recycled and reused after service. This new design concept will be an upsurge to greatly reduce electrical waste [38,39], manufacturing costs, and environmental impact under the requirements of global sustainable development.

2 Experimental section

2.1 Preparation of hydrophilic CNT films (NC-1, NC-2) by *in situ* nitrogen doping

As shown in Figure S1, two kinds of hydrophilic CNT films are fabricated by the CVD method using ferrocene as a catalyst, thiophene as a co-catalyst, ethanol and acetone as carbon sources, and melamine or ammonia bicarbonate as nitrogen sources, respectively. Two CNT films prepared using *in situ* nitrogen doping are, respectively, named NC-1 and NC-2.

2.2 Preparation of hydrophilic CNT films (AC, EC, HC) by thiol-ene click reaction

The PCNT film is modified by three different mercaptans AH, HT-EM, and HT-BM. Taking HT-BM as an example, the preparation process is as follows: (i) the PCNT film is completely impregnated in a solution containing 10 g HT-BM, 10 g DMF, and 0.15 g benzoin dimethyl ether (DMPA) for 20 min in a dark environment. (ii) The infiltrated CNT films are exposed to a 300 W ultraviolet light source in a UWave-2000 reactor to initiate thiol-ene click reaction for 40 min. (iii) The unreacted solution is washed with dimethyl formamide (DMF) to remove unreacted mercaptans. (iv) The CNT film obtained should be washed using DI and dried at 60°C to remove the solvent. Functionalized CNT films are obtained and named HC. Through a similar process, as shown in Figure S2, three CNT films modified by AH, HT-EM, and HT-BM are named AC, EC, and HC, respectively.

2.3 Preparation of hydrophilic CNT film (HNC-2)

Nitrogen doping CNT film (NC-2) was modified using HT-BM to prepare hydrophilic CNT film with high mechanical strength and conductivity *via* thiol-ene click reaction between HT-BM and NC-2, which combines *in situ* nitrogen doping and thiol-ene click reaction. It is named HNC-2.

2.4 Recycling of CNT film

The HNC-2 films are immersed in different acid solutions (CH_3COOH/THF, HCOOH/THF, and H_3PO_4/THF) with the same concentration at 60°C. Additionally, the HNC-2 films are immersed in phosphoric acid solution with different concentrations. The best degradation condition is determined that the HNC-2 films were immersed in 3 mol/L phosphoric acid solution for 3 h at 60°C. The degraded film is washed five times with DI and dried for 1 h at 60°C. The recycled CNT film is immersed in a reaction solution, kept in the dark for 20 min, and then reacted under an ultraviolet reactor for 40 min. The unreacted solution was removed using DMF and dried in a vacuum oven at 60°C for 1 h. The second functionalized CNT film can be prepared by thiol-ene click reaction between recycled CNT films and HT-BM. In a similar way, the CNT films are recycled four times and named R_1, R_2, R_3, and R_4, respectively. Correspondingly, CNT films are degraded four times, and each recycled NC-2 films are named D_1, D_2, D_3, and D_4, respectively. Moreover, NC-2 film is immersed in a 3 mol/L phosphoric acid solution, which is served as a control group. The CNT film treated with phosphoric acid is named PA-NC-2. Similarly, NC-2 film is treated by a solvent (DMF) and named DNC-2.

2.5 Recycling of HT-BM

The HNC-2 films are immersed in 3 mol/L phosphoric acid solution for 3 h at 60°C. The degradation solution is neutralized with 1 mol/L of sodium hydroxide solution and extracted with tetrahydrofuran. Then, we collect the organic phase, add anhydrous sodium sulfate, and let it stand for a night to remove water. Finally, the solvent is removed using spin evaporation, and the yellow degradation product is collected. Yellow degradation product is dissolved in DMF and reacted with slightly excessive formaldehyde solution at 85°C for 5 h. Yellow slime is obtained after removing the solution.

2.6 Closed-loop recycling of CNT film and monomer

NC-2 film is functionalized by HT-BM by thiol-ene click reaction to prepare HNC-2 film. Then, HNC-2 is immersed in 3 mol/L phosphoric acid solution for 3 h at 60°C to obtain recycled NC-2 film. Meanwhile, the degradation solution is neutralized with sodium hydroxide solution, extracted with tetrahydrofuran, dried by anhydrous sodium sulfate and then by spin evaporation to collect recycled monomer, which is reacted with excess formaldehyde solution to obtain recycled HT-BM. Recycled NC-2 film is functionalized by recycled HT-BM to prepare the first cycled functionalized CNT film (C_1). Similarly, the second and third cycled functionalized CNT films are named C_2 and C_3. Concurrently, solvents such as anhydrous ethanol, DMF, and THF are recycled by spin evaporation and reused for the next synthesis or extraction.

3 Results and discussion

3.1 Properties of functionalized CNT films

PCNT film was of strong hydrophobicity and stability (Figure S3a). All of the three mercaptans possessed good wettability (Figure S3b–d) on the PCNT films. Two CNT films prepared by *in situ* nitrogen doping are named NC-1 and NC-2, respectively. *In situ* nitrogen doping can introduce nitrogen atoms into the graphitic structure of the CNT [40,41], causing the transformation of CNT films from hydrophobic to hydrophilic [27,42,43] (Figure S4a and b). Thiol-ene click reaction successfully introduced mercaptans into CNT films to improve the wettability of CNT films (Figure S4c and d). And it was confirmed using Fourier transform infrared (FT-IR), X-ray photoelectron spectroscopy (XPS), and X-ray power diffraction (XRD) in Figures S12–S14 that the thiol-ene click reaction is operated between carbon–carbon double bonds of NC-2 film. Combining the two methods, the thiol-ene click reaction is operated between carbon–carbon double bonds of NC-2 film and thiol group of HT-BM to prepare thiol-functionalized CNT film (HNC-2), whose wettability is the best (Figure S4). Moreover, controllable wettability has been realized by adjusting the amount of mercaptan (Figure S5), which is more simple and energy-saving than traditional plasma treatment [44].

Figure 2a shows the total XPS spectra of the PCNT, NC-2, and HNC-2. PCNT mainly consisted of C and O atoms. The new nitrogen element appeared in NC-2, indicating *in situ* nitrogen doping is successful. Meanwhile, the new sulfur element appeared in HNC-2, confirming

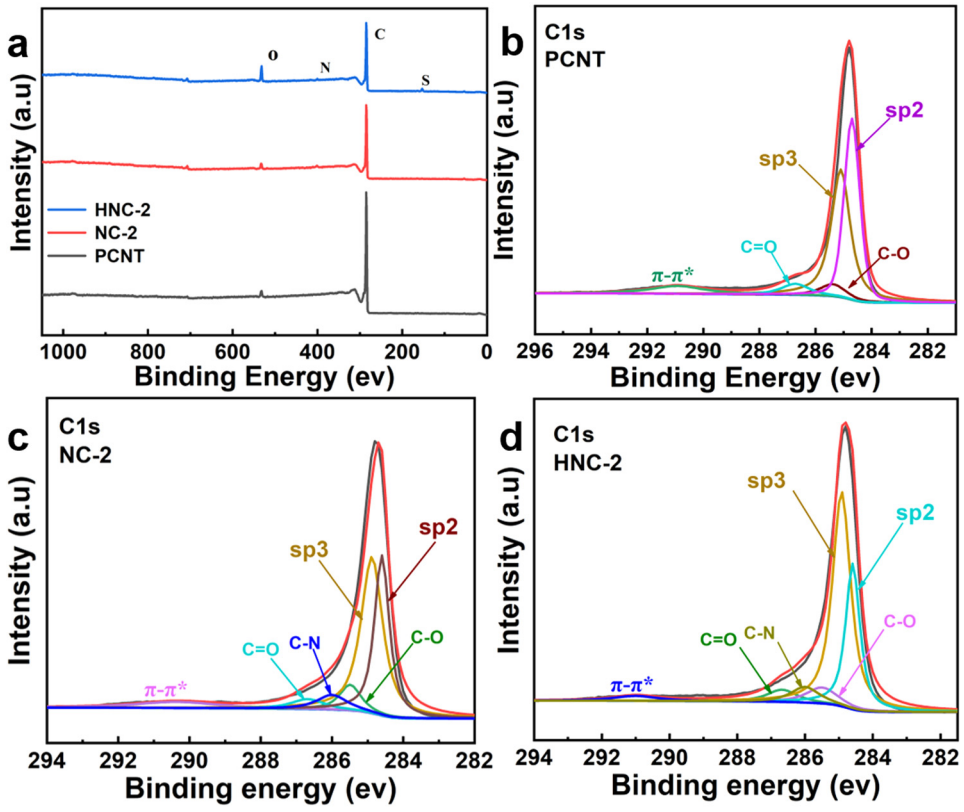

Figure 2: Spectra of PCNT, NC-2, and HNC-2: (a) total XPS and (b–d) C1s XPS.

that the click reaction is successful. Figure 2b shows that the PCNT is composed of five carbon atoms, including C–C (sp^2, 284.6 eV), C–C (sp^3, 285.4 eV), C═O(286.5), C–O(285.6 eV), and π–π* shake-up feature (291.0 eV) [45–48]. From Figure 2c and d C1s XPS, carbon atoms are transferred from sp^2 binding to sp^3 binding by *in situ* nitrogen doping and click reaction, which is proved by a rapid increase of sp^3 phase and a steep decrease of sp^2 in HNC-2, so the ratio of sp^3/sp^2 from 1.55 increase to 2.93. The total spectra of HNC-2, degraded HNC-2 and recycled HNC-2, are shown in Figure 3a. After degradation, the peak of the S element disappeared and the peak of N was maintained. Recycled HNC-2 is similar to the original HNC-2. Therefore, the recycling of HNC-2 is successful. From Figure 3b and c, N1s spectra of NC-2 and HNC-2 indicate that *in situ* nitrogen doping and click reaction achieve the doping of nitrogen. And from the S2p spectra of HNC-2 in Figure 3d, the two peaks at 164.1 and 164.9 eV, corresponding to C–SH and C–S–C [49,50], respectively. The appearance of C–S–C indicates that the thiol-ene click reaction between the thiol group in HT-BM and the double bond in CNTs. The peak of C–SH is due to a small amount of thiol group residues in the HNC-2 after the reaction.

But the effect is limited. XPS explained the low covalent structure and the poor tensile strength very well. The elemental composition of the PCNT and modified films (NC-2 and HNC-2) is shown in Table 1. For the PCNT, a small amount of nitrogen (0.13%) is inherent in CNT [51], and sulfur (0.44%) may come from thiophene used in the preparation of CNT film. And the content of nitrogen in the modification films (NC-2) is 1.46, indicating *in situ* nitrogen doping is successful. The increase in nitrogen and sulfur content is attributed to the click reaction of the sulfhydryl groups in the triazine ring (HT-BM) with the double bonds between the CNTs. The results further certificate that the HT-BM has successfully modified PCNT by thiol-ene click reaction.

As described in Figure 4a, the mechanical property of PCNT film is 22.7 MPa. This is attributed to many particle impurities, large amounts of voids, low orientation, and connections among nanotubes [12]. The mechanical properties and conductivity have been strengthened while the wettability of six functionalized CNT films is improved, which are shown in Figure 4a–c. The tensile stress of six functionalized CNT films (NC-1, NC-2, AC, EC, HC, and HNC-2) increased by 268.72, 367.84, 429.95, 527.31, 633.90, and 1363.00%, respectively. Young's modulus improved 474.19, 532.26, 670.97, 725.81, 925.81, and 1661.60%, respectively. The Raman spectra of PCNT and modified CNT films are described in Figure 4d. The I_D/I_G value of PCNT film was 0.33. After modification, I_D/I_G values of NC-1, NC-2, AC, EC, HC, and HNC-2 are improved to 0.38, 0.40, 0.43, 0.46, 0.48, and 0.56, which indicated that the modification is successful. And we will talk about why successful modification can improve the properties. *In situ* nitrogen doping can improve the mechanical performance of the introduction of nitrogen skeleton.

Weak van der Walls force among PCNTs leads to the poor ability in load transfer and slip. In terms of CNT films functionalized by three mercaptans, highly cross-linked networks between CNTs provided by thiol functional groups in mercaptans contribute to further densification of the CNT films and reduce the slipping between CNTs. And numerous CNTs are interconnected, providing a good bridge of high-efficiency load transfer between nanotubes [52,53], thus causing the increase in tensile strength and Young's modulus. HT-BM shows a more efficient improvement. This is because there are three thiol groups in an HT-BM molecule, immensely increasing the degree of crosslinking, and HT-BM possesses not only a rigid triazine ring structure but also a rigid benzene ring structure, causing its higher tensile stress and Young's modulus than linear mercaptans and aliphatic mercaptans. Moreover, the interaction between CNTs can be enhanced by π–π stacking [54] as XPS spectra showed.

The enhancement of high performance is not only mechanical performance but also electrical conductivity in Figure 4c. The electrical conductivity of PCNT film is 161.60 and 211.90 S/cm in perpendicular and longitudinal directions. The electrical conductivity of NC-1 and NC-2 is increased by 45.98 and 56.99% in the perpendicular direction, 51.39 and 69.98% in the longitudinal direction, respectively. More electronic transmission channels are provided with the introduction of nitrogen, and the improvement of wettability is beneficial for electron migration. Similarly, the thiol-ene click reaction creates substantial cross-linked networks and contact number, which enhances the interaction and increases the number of conductive networks and electronic transmission channels between CNTs. AC, EC, and HC are equipped with excellent conductivity through chemical crosslinking, as exhibited in Figure 4c. Their conductivity is promoted by 95.97, 111.32, and 134.47% in a perpendicular direction and 96.03, 107.36, and 121.23% in the longitudinal direction, respectively. HT-BM is more efficient than monothiol and HT-EM as a consequence of higher cross-linked networks, and more electronic transmission channels between CNTs. HNC-2 film shows the best properties (high mechanical strength and high conductivity) under the combined action of the two doping ways.

Raman spectra of PCNT film and functionalized films are shown in Figure 4d. The peaks at 1,330 and 1,580 cm^{-1}

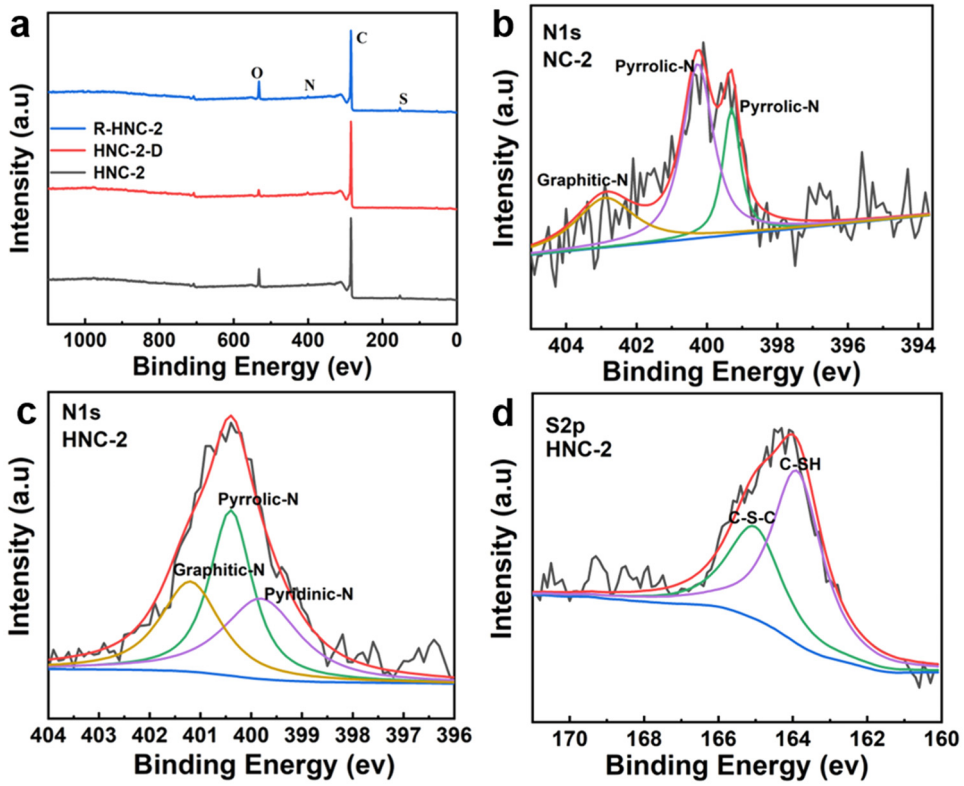

Figure 3: Spectra of HNC-2, HNC-2-D, and R-HNC-2: (a) total XPS, (b) N1s XPS of NC-2, (c) N1s of HNC-2, and (d) S2p of HNC-2.

Table 1: Element analysis results of PCNT and modified films (NC-2, HNC-2)

Sample	C (wt%)	O (wt%)	N (wt%)	S (wt%)
PCNT	97.10	2.33	0.13	0.44
NC-2	96.18	2.09	1.46	0.27
HNC-2	87.07	1.98	3.82	7.13

are both carbon crystal peaks and belong to the D-band and the G-band, respectively. D-Band implies the defects of carbon crystal, and G peak is a distinct character from the tangential vibration modes of sp^2 bound carbon atoms in graphitic materials. The standard for measuring the degree of defects of CNT films is the integrated intensity ratio between D and G bands, which is indicative of the defect degree in the graphitic lattice. Compared with PCNT films, the integrated intensity ratio between D and G bands is increased from 0.33 (PCNT) to 0.38 (NC-1), 0.40 (NC-2), 0.43 (AC), 0.46 (EC), 0.48 (HC), and 0.56 (HNC-2), respectively. The I_D/I_G values for NC-1 and NC-2 are both higher than those for PCNT film, indicating that more defects and disorders in graphitic layers have been aroused with the *in situ* doping of nitrogen. In addition, the obvious higher I_D/I_G value for thiol-functionalized CNT films suggests an increased presence of defects and disorders in the CNT films. Thiol groups of mercaptans react with the double bond of the CNTs, resulting in the carbon atoms being transferred from sp^2 bound into sp^3 bound. The results demonstrate the successful modifications.

In order to confirm the functionalized CNT film can be adjustable to the temperature of almost all electronic equipment applications, the stress relaxation experiment was conducted at 60°C. The stress relaxation curve of PCNT, NC-2, and HNC-2 films is shown in Figure S7a. HNC-2 possesses higher mechanical performance and strength retention during relaxation. And there is a synergistic effect between stress and strength retention during relaxation.

Not only the performance but also the micrographs of modified CNT film showed a great difference. PCNT is loose, more disordered, and with many holes (Figure 5a). Differently, many flaky materials on scanning electron microscopic (SEM) micrographs of NC-1 and NC-2 in Figure 5b and c appeared but not in PCNT, indicating that nitrogen atoms are successfully introduced into CNTs. And XPS of PCNT, NC-1, and NC-2 in Supplementary materials (Figure S15) further confirmed it. In addition, there are slight differences in the surface between NC-1 and NC-2 because of the change

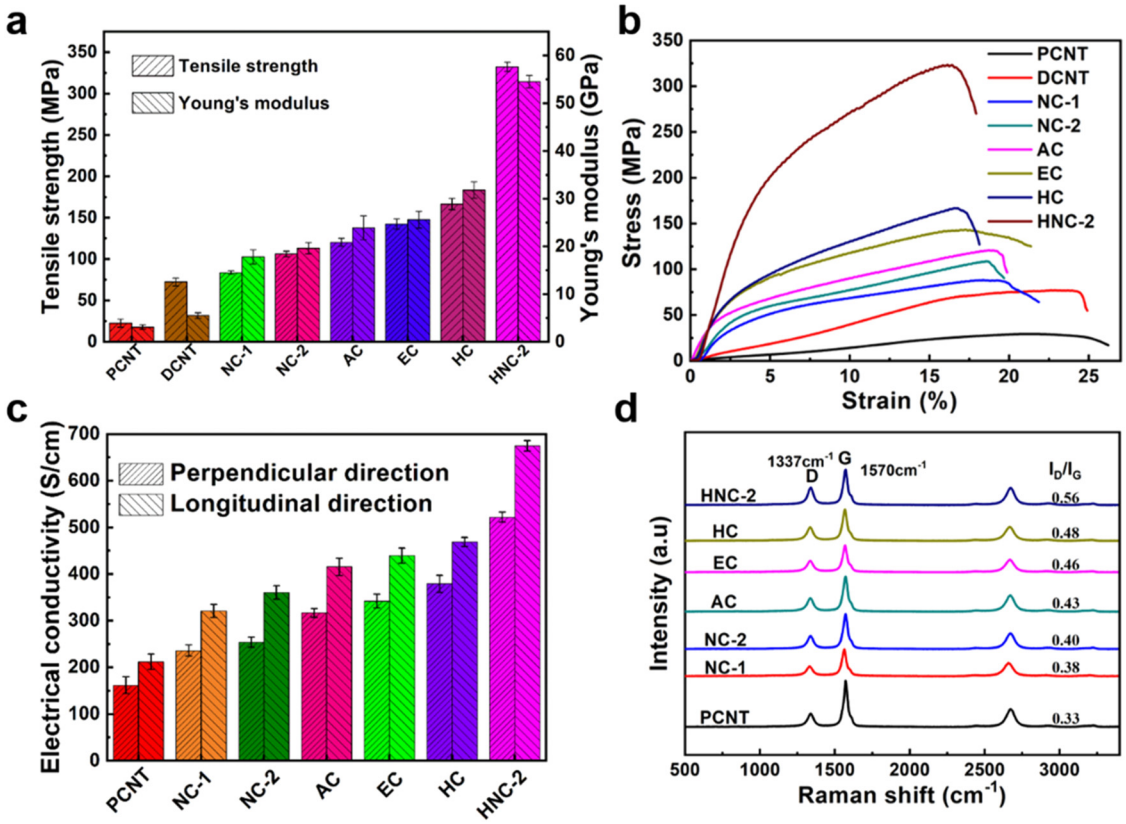

Figure 4: Properties of pristine and modified CNT films: (a) tensile strength, (b) stress–strain curves, (c) electrical conductivity, and (d) Raman spectra.

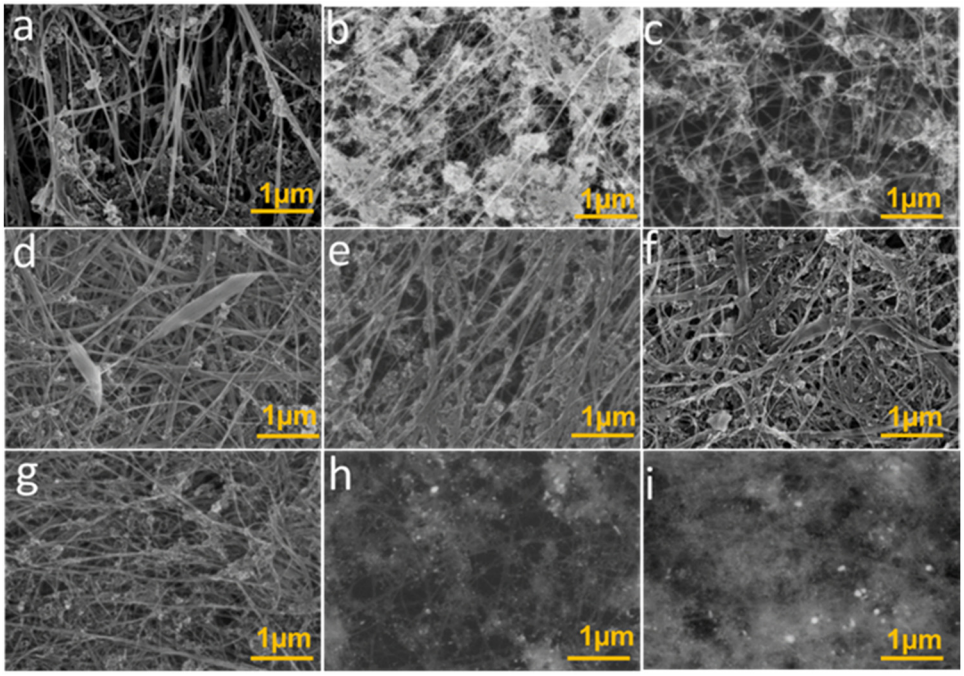

Figure 5: SEM micrographs of CNT films with lower magnification: (a) PCNT, (b) NC-1, (c) NC-2, (d) AC, (e) EC, (f) HC, (g) HNC-2, (h and i) backscattered electron imaging of NC-2 and HNC-2.

in nitrogen sources [55] (melamine and ammonia bicarbonate). The last three micrographs (Figure 5d–f) belong to CNT films functionalized by three different mercaptans. Compared with PCNT film, the thiol-functionalized CNT films become more compact, in which CNTs are connected to each other more tightly, and coated by mercaptans [56]. The obvious changes imply that CNT film is successfully functionalized *via* thiol-ene click reaction. Meanwhile, the SEM image of HNC-2 film keeps the characteristics of CNT film functionalized by both *in situ* nitrogen doping and thiol-ene click reaction. Moreover, backscattered electron imaging of NC-2 and HNC-2 is conducted (Figure 5h and i). The image of NC-2 is mainly dark, indicating the main component is carbon. A small amount of bright spots belongs to nitrogen by *in situ* doping and catalyst impurities such as iron and sulfur whose relative atomic mass is larger than that of carbon. The image of HNC-2 is mainly bright, implying many substances larger than carbon atoms are reacted on CNT films by *in situ* nitrogen doping and thiol-ene click reaction. From SEM micrographs of CNT films with higher magnification, PCNT is more desperate, and there is no cross-linking between CNTs in Figure 6a. Nitrogen doping enhanced the connection of CNTs as shown in Figure 6b and c. After PCNT is functionalized by thiol-ene click reaction, thiol-functionalized CNT films were covered with HT-BM polymers, and a large number of voids in the original PCNTF were filled up as shown in Figure 6d and e. This supports the appointment that HT-BM provides an effective load transfer among the CNTs, which in turn increases the tensile strength of the functionalized film. In Figure 6f, SEM micrographs show the double features of nitrogen doping and thiol-ene click reaction in surface appearance. Because of the joint enhancement of the two, HNC-2 shows high performance, which is consistent with the former conclusions.

3.2 Recycling of CNT film and monomer

It was reported that hexahydrotriazine had good degradation cycle performance [57]. Due to the thiol-ene click reaction introducing the degradable structure of hexahydro-s-triazine (HT), HNC-2 films can realize recovery by acid treatment. In order to overcome the problem that monomers cannot be recycled in strong acid degradation, three weak acids are selected. As Figure 7a shows that the degradation rate of the functionalized CNT film (HNC-2) is the fastest under phosphoric acid compared with formic acid and acetic acid at the same concentration. This is because phosphoric acid can provide more hydrogen ions. Then, functionalized CNT film is degraded under different concentrations of phosphoric acid solution. The degradation degree almost reaches saturation in about 3 h under the concentration of either 3 or 3.5 mol/L (Figure 7b). In terms of safety and cost, 3 mol/L was chosen as the better condition. From Figure 7c, the influence of degradation ratio in different mass ratios of CNT films to phosphoric acid solution has been researched; 1:250 mass ratio has higher degradation rate than the higher mass ratio of CNT films to the phosphoric acid solution. This is because the degradation ability of a certain amount of phosphoric acid is limited. Before the 1:250 mass ratio, the degradation ratio is improved with the increase of the mass of phosphoric acid. And

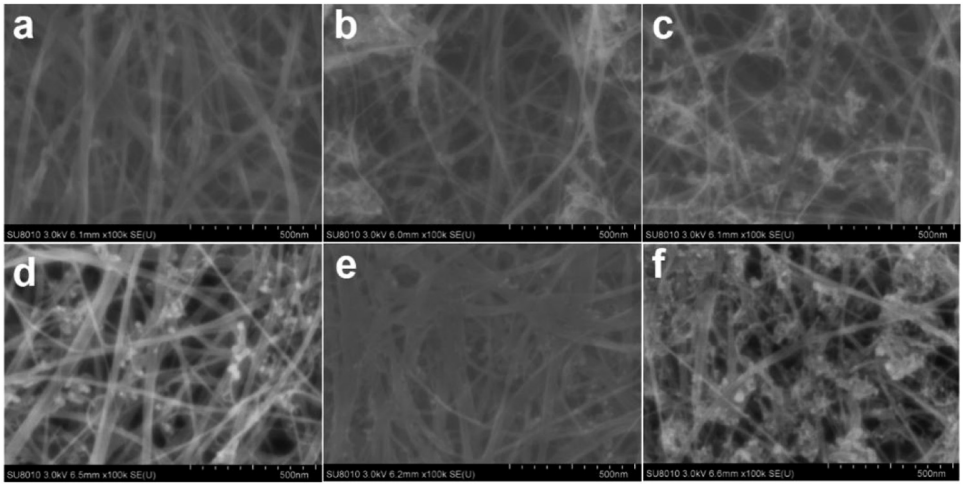

Figure 6: SEM micrographs of CNT films with higher magnification: (a) PCNT, (b) NC-1, (c) NC-2, (d) EC, (e) HC, and (f) HNC-2.

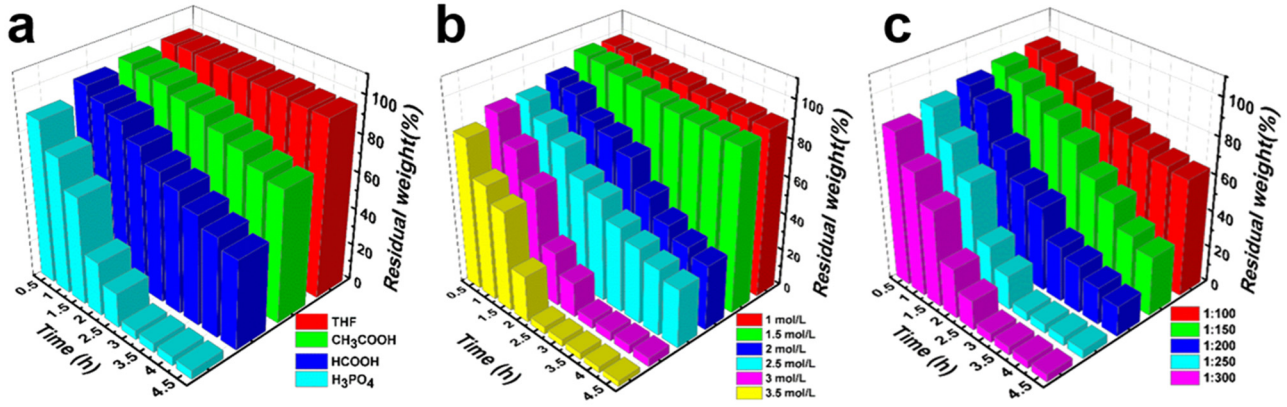

Figure 7: The effect of different conditions on the degree of mercaptan degradation: (a) the type of acids, (b) concentration of acids, and (c) the mass ratio of CNT films to the acid solution.

hydrogen ions and water gradually infiltrated into hydrophilic CNT film to improve the degradation ratio. When the mass ratio reached a saturated degree, the amount of hydrogen and water is no longer an obvious factor. So 1:250 and 1:300 mass ratios have equal degradation rates.

In Figure 8a, the tensile strength of HNC-2 is about 332.3 MPa. After degradation, the tensile strength is reduced to 126.1 MPa, which is higher than that of NC-2 (106.2 MPa). But the strength is really close to that of NC-2 with the treatment of DMF. In addition, the elongation at the break is also consistent with that of NC-2. Therefore, NC-2 films have good cyclic performance. Moreover, the tensile strength of PA-NC-2 (NC-2 by phosphoric acid treatment) was 144.7 MPa, but the elongation at

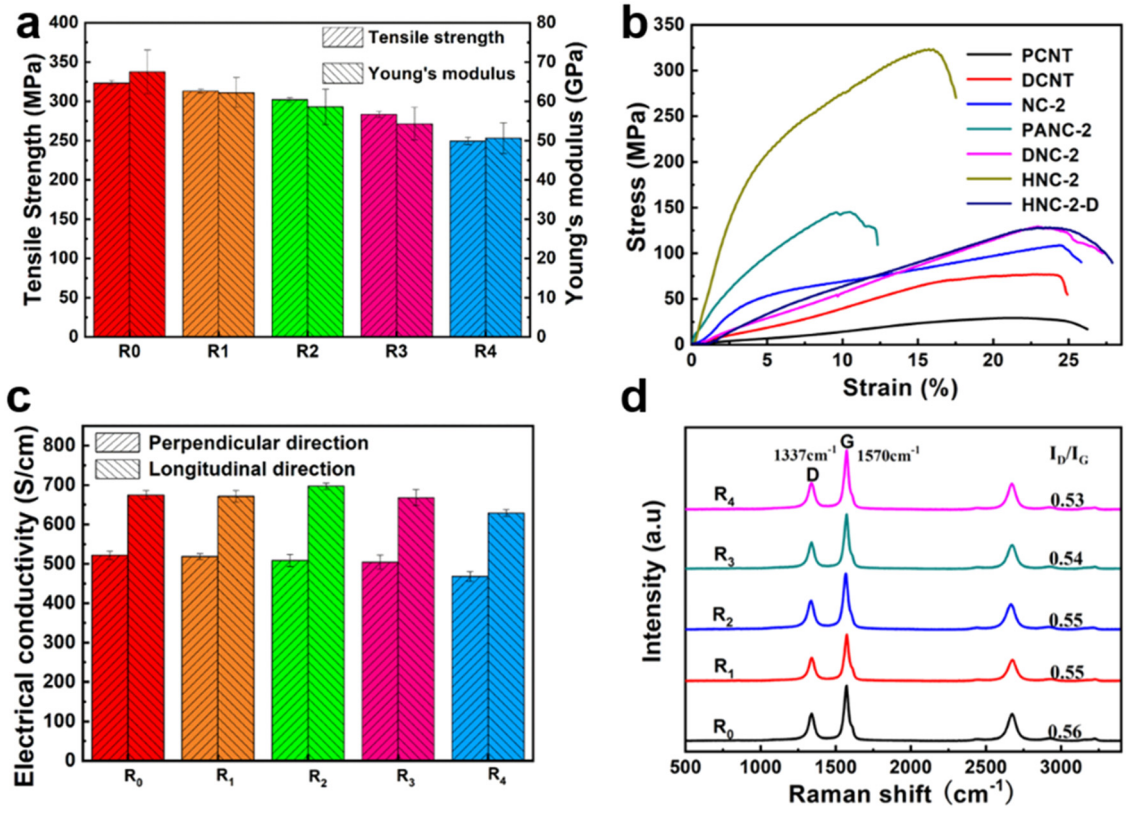

Figure 8: The properties of recovered CNT films functionalized by recycled NC-2 and HT-BM: (a) stress–strain curve of CNT films by different treatment, (b) electrical conductivity, (c) tensile strength, and (d) Raman spectra.

the break is reduced to 9.5%. Therefore, the tensile stress of recycled CNT film higher than NC-2 is caused by solvent treatment, further indicating that NC-2 film is successfully recycled.

Additionally, the recycled CNT film is functionalized by HT-BM to obtain recycled thiol-functionalized CNT film four times. The tensile strength and electrical conductivity of recycled functionalized CNT film every time are shown in Figure 8b and c. The tensile strength has a high retention rate, and still maintains 84% after four cycles, while electrical conductivity did not decrease significantly. Moreover, the Raman spectra of every functionalized CNT film are exhibited in Figure 8d. I_D/I_G is equal, indicating recycled thiol-functionalized CNT films have similar defects. In terms of SEM micrographs of thiol-functionalized CNT film (R_0) and the last recycled CNT film (R_4) (Figure S8), almost no change has happened, indicating that closed-loop recycling of CNT film is successful.

On the contrary, the tensile strength and electrical conductivity of successively recycled CNT films (D_1, D_2, D_3, and D_4) are shown in Figure 9a and b. The tensile strength of recycled CNT films is unchanged basically, and similar to DNC-2 (NC-2 treated with DMF), implying that NC-2 film possesses cyclic robustness. Cyclic robustness is also shown in electrical conductivity. As shown in Figure 9c, the Raman spectra of recycled CNT films are similar, and the value of I_D/I_G of them is 0.40 or 0.41, which is consistent with that of NC-2 film.

From the TGA curves of CNT films with different treatments in Figure 9d, the TGA curve of *in situ* nitrogen doping CNT film is horizontal, implying that it possesses good thermal stability. After modification of the thiol-ene click reaction, HNC-2 films began to lose weight at about 200°C. The rate of weight loss is about 26%, which is attributed to the decomposition of organic compounds. It is confirmed that the mercaptan successfully reacted on the CNT film. After degradation of functionalized CNT film (HNC-2), the TGA curve of the recycled CNT film is similar to that of NC-2, indicating resin is degraded. The recycled CNT film is functionalized by HT-BM, and the TGA curve of functionalized CNT film in the fourth cycle is shown. The rate of weight loss recovers to about 27%, implying that the recycled CNT film possesses good cyclical stability, and can be functionalized four times. The weight loss of CNT film after the fourth degradation is

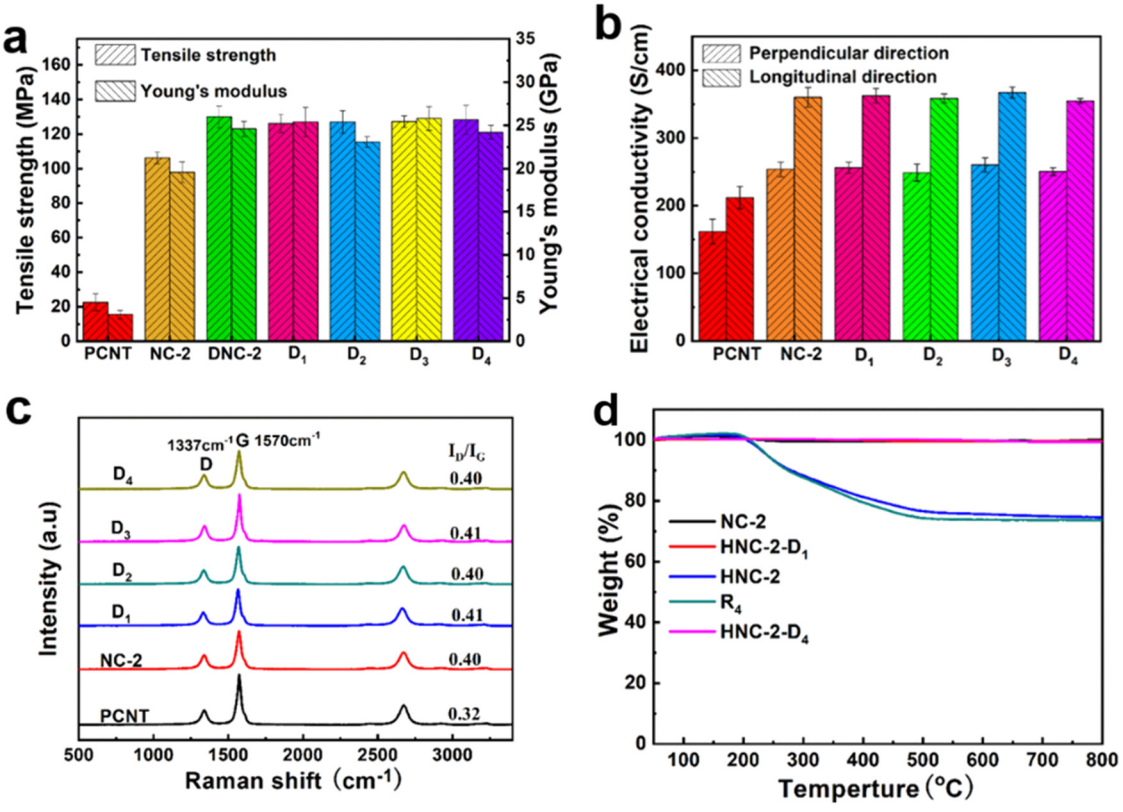

Figure 9: Properties of recycled *in situ* nitrogen doped CNT film: (a) the strength of CNT films, (b) electrical conductivity of CNT films, (c) Raman spectra of recycled NC-2 films, and (d) TGA curves of treated CNT films.

close to that of NC-2. It is confirmed that the functionalized CNT films are recycled successfully. And SEM micrographs of CNT film after the fourth degradation are really close to that of pristine NC-2 (Figure S9), indicating that phosphoric acid solution causes no great damage to NC-2 film, *in situ* nitrogen-doped CNT film is stable and recyclable.

Degradation product is obtained after neutralization, extraction, and drying, and was characterized by gas chromatograph-mass spectrometry. As shown in Figure S10a, there is only one peak at the retention time of 10.66 min. And molecular weight is 125. The structure was simulated to be 2-aminobenzenethiol. FT-IR spectra of recycled monomer are consistent with the original monomer (2-aminobenzenethiol) in Figure S10b. Moreover, the ^{1}H-NMR spectrum of it is shown in Figure S10c. The ratio of the peak area of the hydrogen atom spectrum is similar to the ratio of the number of hydrogen atoms in the molecular structure, indicating that 2-aminobenzenethiol has been recycled. And the recycling rate of 2-aminobenzenethiol is 86.72%.

When adding excessive formaldehyde, mercaptan can be synthesized in DMF solution, which is characterized by FT-IR (Figure 10a). For the degradation product of HNC-2, the absorption peak at 1,237 cm^{-1} attributed to –NH of hexahydro-s-triazine (HT) disappeared, demonstrating the successful degradation. The degradation product is reacted with formaldehyde. The absorption peak of recycled HT-BM is consistent with original mercaptan (HT-BM), indicating HT-BM has been resynthesized successfully. ^{1}H-NMR spectra of HT-BM are shown in Figure 10b. The peaks at 7.11 ppm (d), 7.00 ppm (b), 6.78 ppm (c), and 6.65 ppm (b) are attributed to the chemical shift of hydrogen atom in –CH– of the benzene ring. The peak at 4.83 ppm (e) is attributed to the chemical shift of hydrogen atoms in –CH_2– in the HT, and the peak at 4.56 ppm (f) belongs to the chemical shift of hydrogen atom –SH attached to the benzene ring. The peak of the solvent chloroform appeared at 7.26 ppm (g). The ratio of the peak area of the hydrogen atoms is corresponding to the ratio of the number of hydrogen atoms, indicating that the mercaptan (HT-BM) has been recycled successfully. And the recycling rate of HT-BM is 87.16%. Recycled HT-BM is reused to modify recycled NC-2 film. FT-IR spectra of recycled NC-2 film, recycled HT-BM, and recycled HNC-2 film are exhibited in Figure 10c. The peak at 2,613 cm^{-1} (–SH) in recycled HT-BM is obvious, while the peak at 2,613 cm^{-1} (–SH) in thiol-functionalized CNT film is weak,

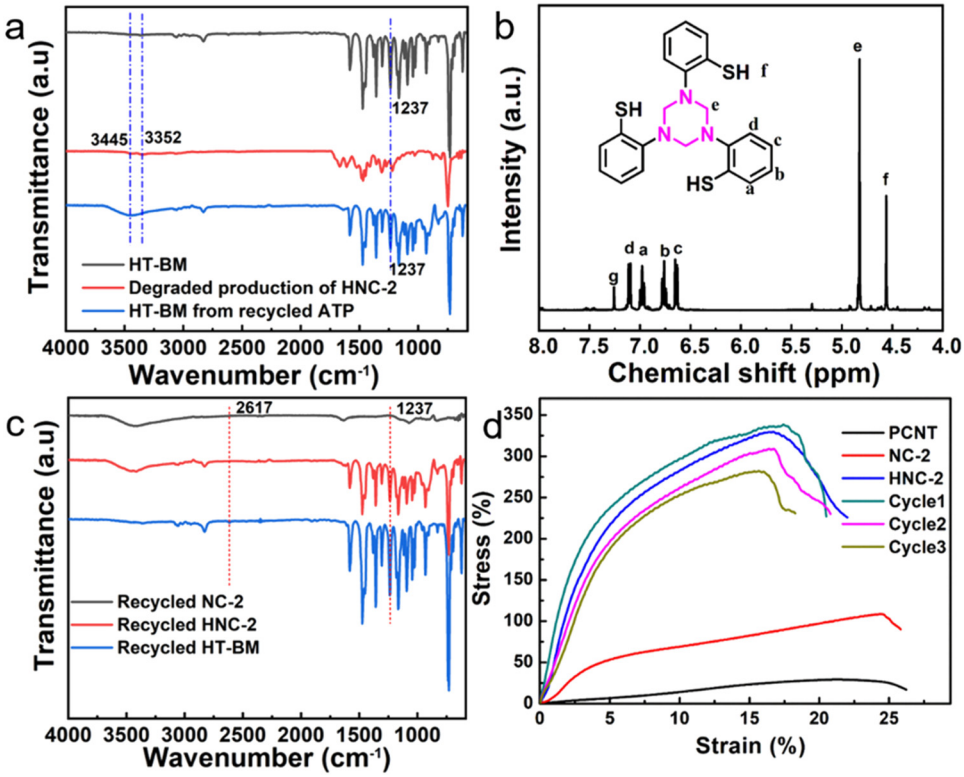

Figure 10: Properties of monomer and recovered thiol-functionalized CNT film: (a) FT-IR spectra of a chemical compound, (b) ^{1}H-NMR of a chemical compound, (c) FT-IR spectra of modified CNT film, and (d) stress–strain curves of recovered CNT films.

demonstrating the occurrence of thiol-ene click reaction between the thiol group of recycled HT-BM and double bond of recycled NC-2. The absorption peaks of recycled HNC-2 are greatly different from that of recycled NC-2 film, and the absorption peak at 1,237 cm^{-1} attributed to C–N of hexahydro-s-triazine structure appeared in recovered HNC-2 film, indicating that recycled HT-BM has grafted on recycled NC-2. This also suggests the fact that NC-2 is functionalized by HT-BM successfully. The mechanical properties of recovered functionalized CNT film by recycled CNT film and recycled HT-BM are shown in Figure 10d. Functionalized CNT film is degraded and regenerated by reacting with recycled mercaptan, which possesses equal strength to pristine thiol-functionalized CNT film (HNC-2). And the operation is repeated three times with a higher retention rate (over 80%) in mechanical performance. Our closed-loop recycling of CNT film and monomer is superior to common electrochemical degradation [28] and physical closed-loop recovery [58]. The mechanism of fabricating functionalized CNT film is *in situ* nitrogen doping and thiol-ene click reaction which is occurred between carbon–carbon double bond of NC-2 film and thiol group of HT-BM. The mechanism of the degradation cycle of functionalized CNT film is that the hexahydro-s-triazine ring of HT-BM is destroyed by hydrogen ions and water molecules. After neutralization, extraction, and drying, monomer (2-aminobenzenethiol) is obtained. Adding formaldehyde solution, a condensation reaction is conducted between amino groups of recycled 2-aminobenzenethiol and aldehyde groups of formaldehyde. Hexahydro-s-triazine ring is recovered by removing molecules of water. Therefore, mercaptan (HT-BM) is recycled with a recycling rate of 87.16%, which can react with recycled NC-2 films by thiol-ene click reaction again. And recycled NC-2 has equal performance, value of I_D/I_G, and TGA curve to pristine NC-2. Thus, the mechanism of recycling CNT film may be the crack of sulfide bond in acid environment and 60°C. This is the mechanism of closed-loop recycling of CNT film and mercaptan (HT-BM). The mechanism of closed-loop recycling of CNT film and monomer is shown in Figure 11.

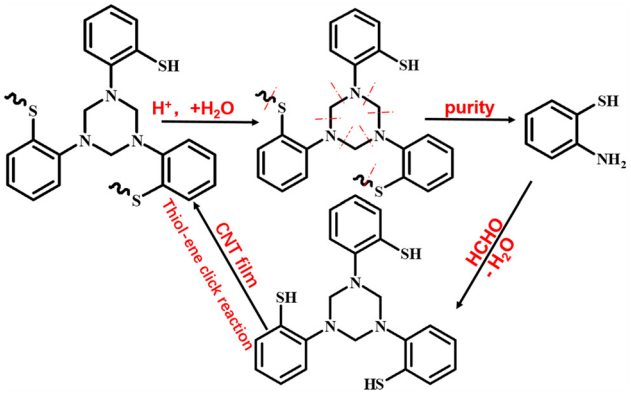

Figure 11: The mechanism of preparation and degradation cycle of nitrogen-doped CNT film functionalized by hexahydro-s-triazine.

4 Conclusion

In summary, the hydrophobic PCNT film was obtained through *in situ* nitrogen doping to improve the interaction among CNTs. Then, the NC-2 film was functionalized by thiol-ene click reaction with mercaptan (HT-BM) containing degradable hexahydro-s-triazine to prepare thiol-functionalized CNT film (HNC-2). Due to the covalent crosslinking between CNTs and the rigid structure of the triazine ring, the HNC-2 exhibited remarkable improvements in controllable wettability, mechanical performance (332 MPa), as well as electrical conductivity (675 S/cm). The results of Raman spectra, TGA curves, and SEM images indicated that CNT films were functionalized, degraded, and closed-loop recycled successfully. Furthermore, the HNC-2 could be degraded into monomer and CNT films again. The recycled monomer could be utilized as feedstock to react with formaldehyde in the DMF solution to prepare new HT-BM, delivering recyclability as high as 86.72 and 87.16%, respectively. The NC-2 can achieve recyclability of almost 100% and could be used to fabricate new thiol-functionalized CNT film without apparent deterioration in mechanical and electrical performance. The thiol-functionalized CNT film system realized closed-loop recycling of both monomer and CNT film. Great advantages in the reuse of CNT films and monomers were shown, such as saving resources, protecting environment, and reducing costs. This work provides an environmentally sustainable approach for designing degradable thiol-functionalized CNT film to address the resource waste and cancer risk of CNTs as a consequence of the annual consumption of billions of tons of CNTs without recycling. From the perspective of environment protection and resource conservation, closed-loop recycling of CNT films and monomers is the most efficient way to solve these problems. And it will provide new materials and new design concepts for CNT-film-based battery and capacitor research.

Acknowledgments: The authors acknowledge financial support from the National Natural Science Foundation of China (51873233), Innovation Group of National Ethnic Affairs Commission of China (MZR20006), Key R & D Plan of Hubei Province (2020BAB077), and Fundamental Research Funds for the Central Universities (CZP20006).

Funding information: National Natural Science Foundation of China (51873233), Innovation Group of National Ethnic Affairs Commission of China (MZR20006), Key R & D Plan of Hubei Province (2020BAB077), and Fundamental Research Funds for the Central Universities (CZP20006).

Author contributions: All authors have accepted responsibility for the entire content of this manuscript and approved its submission.

Conflict of interest: The authors state there is no conflict of interest.

References

[1] Iijima S. Helical microtubules of graphitic carbon. Nature. 1991;354(6348):56–8. doi: 10.1038/354056a0.
[2] Rdest M, Janas D. Carbon nanotube films for energy applications. Energies. 2021;14(7):1890. doi: 10.3390/en14071890.
[3] Wang QF, Ran X, Shao WK, Miao MH, Zhang DH. High performance flexible supercapacitor based on metal-organic-framework derived CoSe2 nanosheets on carbon nanotube film. J Power Sources. 2021;490:229517. doi: 10.1016/j.jpowsour.2021.229517.
[4] Mirvakili SM, Hunter IW. Artificial muscles: mechanisms, applications, and challenges. Adv Mater. 2018;30(6):1704407. doi: 10.1002/adma.201704407.
[5] Zhou Y, Zhan P, Ren M, Zheng G, Dai K, Mi L, et al. Significant stretchability enhancement of a crack-based strain sensor combined with high sensitivity and superior durability for motion monitoring. ACS Appl Mater Interfaces. 2019;11(7):7405–14. doi: 10.1021/acsami.8b20768.
[6] Zhou W, Shen H, Wang Q, Onoe J, Kawazoe Y, Jena P. N-doped peanut-shaped carbon nanotubes for efficient CO2 electrocatalytic reduction. Carbon. 2019;152:241–6. doi: 10.1016/j.carbon.2019.05.078.
[7] Zhao X, Cheng L, Wang R, Jia N, Liu L, Gao C. Bioinspired synthesis of polyzwitterion/titania functionalized carbon nanotube membrane with superwetting property for efficient oil-in-water emulsion separation. J Membr Sci. 2019;589:117257. doi: 10.1016/j.memsci.2019.117257.
[8] Ma Y, Lv C, Tong Z, Zhao CF, Li YS, Hu YY, et al. Single-layer copper particles integrated with a carbon nanotube film for flexible electromagnetic interference shielding. J Mater Chem. 2020;8(29):9945–53. doi: 10.1039/d0tc02087g.
[9] Gohardani O, Elola MC, Elizetxea C. Potential and prospective implementation of carbon nanotubes on next generation aircraft and space vehicles: A review of current and expected applications in aerospace sciences. Prog Aerosp Sci. 2014;70:42–68. doi: 10.1016/j.paerosci.2014.05.002.
[10] Yang L, Cui J, Zhang L, Xu X, Chen X, Sun DA. Moisture-driven actuator based on polydopamine-modified MXene/bacterial cellulose nanofiber composite film. Adv Funct Mater. 2021;31(27):2101378. doi: 10.1002/adfm.202101378.
[11] Adusei PK, Gbordzoe S, Kanakaraj SN, Hsieh YY, Alvarez NT, Fang Y, et al. Fabrication and study of supercapacitor electrodes based on oxygen plasma functionalized carbon nanotube fibers. J Energy Chem. 2020;40:120–31. doi: 10.1016/j.jechem.2019.03.005.
[12] Duan Q, Wang Y, Chen S, Miao M, Chen S, Zhang D. Functionalized carbon nanotube films by thiol-ene click reaction. Appl Surf Sci. 2019;486:144–52. doi: 10.1016/j.apsusc.2019.05.011.
[13] Zou H, Li X, Zhang Y, Wang Z, Zhuo B, Yuan Q, et al. Effects of different hot pressing processes and NFC/GO/CNT composite proportions on the performance of conductive membranes. Mater Design. 2021;198:109334. doi: 10.1016/j.matdes.2020.109334.
[14] Wang JN, Luo XG, Wu T, Chen Y. High-strength carbon nanotube fibre-like ribbon with high ductility and high electrical conductivity. Nat Commun. 2014;5:3848. doi: 10.1038/ncomms4848.
[15] Feng L, Wu R, Liu C, Lan J, Lin YH, Yang X. Facile green vacuum-assisted method for polyaniline/SWCNT hybrid films with enhanced thermoelectric performance by interfacial morphology control. ACS Appl Energy Mater. 2021;4(4):4081–9. doi: 10.1021/acsaem.1c00419.
[16] Jung Y, Kim T, Park CR. Effect of polymer infiltration on structure and properties of carbon nanotube yarns. Carbon. 2015;88:60–9. doi: 10.1016/j.carbon.2015.02.065.
[17] Rahimpour A, Jahanshahi M, Rajaeian B, Rahimnejad M. TiO2 entrapped nano-composite PVDF/SPES membranes: Preparation, characterization, antifouling and antibacterial properties. Desalination. 2011;278(1–3):343–53. doi: 10.1016/j.desal.2011.05.049.
[18] Hanizam H, Salleh MS, Omar MZ, Sulong AB. Optimisation of mechanical stir casting parameters for fabrication of carbon nanotubes–aluminium alloy composite through taguchi method. J Mater Res and Technol. 2019;8(2):2223–31. doi: 10.1016/j.jmrt.2019.02.008.
[19] Tankus KA, Issman L, Stolov M, Freger V. Electrotreated carbon nanotube membranes for facile oil–water separations. ACS Appl Nano Mater. 2018;1(5):2057–61. doi: 10.1021/acsanm.8b00442.
[20] Wei H, Zhan H, Wang Y, Gu Y, Wang S, Zhang Z, et al. Impacts from the stacking morphology on the tensile performance of double-walled carbon nanotube bundles. Carbon. 2021;178:345–54. doi: 10.1016/j.carbon.2021.03.023.
[21] Sun XL, Liu Z, Cheng ZL. A flexible N-doped carbon-nanofiber film reinforced by halloysite nanotubes(HNTs) for adsorptive desulfurization. J Hazard Mater. 2021;403:123851. doi: 10.1016/j.jhazmat.2020.123851.
[22] Lv X, Yin S. CoP-embedded nitrogen and phosphorus co-doped mesoporous carbon nanotube for efficient hydrogen evolution. Appl Surf Sci. 2021;537:147834. doi: 10.1016/j.apsusc.2020.147834.
[23] Liu SQ, Gao MR, Feng RF, Gong L, Zeng H, Luo JL. Electronic delocalization of bismuth oxide induced by sulfur doping for efficient CO_2 electroreduction to formate. ACS Catal. 2021;11(12):7604–12. doi: 10.1021/acscatal.1c01899.
[24] Pham VL, Kim DG, Ko SO. Catalytic degradation of acetaminophen by Fe and N Co-doped multi-walled carbon nanotubes. Environ Res. 2021;201:111535. doi: 10.1016/j.envres.2021.111535.

[25] Li P, Guo X, Zang R, Wang S, Zuo Y, Man Z, et al. Nanoconfined SnO2/SnSe2 heterostructures in N-doped carbon nanotubes for high-performance sodium-ion batteries. Chem Eng J. 2021;418:129501. doi: 10.1016/j.cej.2021.129501.
[26] Mardle P, Ji X, Wu J, Guan S, Dong H, Du S. Thin film electrodes from Pt nanorods supported on aligned N-CNTs for proton exchange membrane fuel cells. Appl Catal B: Environ. 2020;260:118031. doi: 10.1016/j.apcatb.2019.118031.
[27] Wu M, Zhang G, Chen N, Hu Y, Regier T, Rawach D, et al. Self-reconstruction of Co/Co2P heterojunctions confined in N-doped carbon nanotubes for Zinc–Air flow batteries. ACS Energy Lett. 2021;6(4):1153–61. doi: 10.1021/acsenergylett.1c00037.
[28] Reipa V, Hanna SK, Urbas A, Sander L, Elliott J, Conny J, et al. Efficient electrochemical degradation of multiwall carbon nanotubes. J Hazard Mater. 2018;354:275–82. doi: 10.1016/j.jhazmat.2018.04.065.
[29] Geng Z, Shin JJ, Xi Y, Hawker CJ. Click chemistry strategies for the accelerated synthesis of functional macromolecules. J Polym Sci. 2021;59(11):963–1042. doi: 10.1002/pol.20210126.
[30] Ma X, Xu H, Xu Z, Jiang Y, Chen S, Cheng J, et al. Closed-loop recycling of both resin and fiber from high-performance thermoset epoxy/carbon fiber composites. ACS Macro Lett. 2021;10:1113–8. doi: 10.1021/acsmacrolett.1c00437.
[31] Liu Y, Wang B, Ma S, Yu T, Xu X, Li Q, et al. Catalyst-free malleable, degradable, bio-based epoxy thermosets and its application in recyclable carbon fiber composites. Compos Part B. 2021;211:108654. doi: 10.1016/j.compositesb.2021.108654.
[32] Yu K, Shi Q, Dun M, Wang T, Qi H. Carbon fiber reinforced thermoset composite with near 100% recyclability. Adv Funct Mater. 2016;26(33):6098–106. doi: 10.1002/adfm.201602056.
[33] Liu F, Chen X, Liu H, Zhao J, Xi M, Xiao H, et al. High-yield and low-cost separation of high-purity semiconducting single-walled carbon nanotubes with closed-loop recycling of raw materials and solvents. Nano Res. 2021;14:4281–7. doi: 10.1007/s12274-021-3671-x.
[34] Zou G, Jain M, Yang H, Zhang Y, Williams D, Ji Q. Recyclable and electrically conducting carbon nanotube composite films. Nanoscale. 2010;2:418–22. doi: 10.1039/b9nr00257j.
[35] Ma X, Guo W, Chen S, Cheng J, Zhang J, Miao M, et al. Synthesis of degradable hyperbranched epoxy resins with high tensile, elongation, modulus and low-temperature resistance. Compos Part B. 2020;192:108005. doi: 10.1016/j.compositesb.2020.108005.
[36] Ma X, Liang Y, Xu Z, Chen S, Cheng J, Miao M, et al. The versatility of hyperbranched epoxy resins containing hexahydro-s-triazine on diglycidyl ether of bisphenol-A composites. Compos Part B. 2020;196:108109. doi: 10.1016/j.compositesb.2020.108109.
[37] Guo W, Chen S, Cheng J, Zhang J, Miao M, Zhang D. Synthesis of renewable and self-curable thermosetting hyperbranched polymers by a click reaction. Prog Org Coat. 2019;134:189–96. doi: 10.1016/j.porgcoat.2019.05.009.
[38] Miao J, Liu H, Li Y, Zhang X. Biodegradable transparent substrate based on edible starch-chitosan embedded with nature-inspired three-dimensionally interconnected conductive nanocomposites for wearable green electronics. ACS Appl Mater Interfaces. 2018;10(27):23037–47. doi: 10.1021/acsami.8b04291.
[39] Li J, Zeng X, Sevels A. Ecodesign in consumer electronics: past, present, and future. Crit Reviews Env Sci Tec. 2015;45(8):840–60. doi: 10.1080/10643389.2014.900245.
[40] Hao X, Jiang Z, Zhang B, Tian X, Song C, Wang L, et al. N-Doped carbon nanotubes derived from graphene oxide with embedment of FeCo nanoparticles as bifunctional air electrode for rechargeable liquid and flexible all-solid-state zinc-air batteries. Adv Sci. 2021;8(10):2004572. doi: 10.1002/advs.202004572.
[41] Szabó A, Gyulavári T, Tóth ZR, Pápa Z, Budai J, Hernadi K. The effect of various substrates and catalyst layer deposition on the incorporation of nitrogen into carbon nanotube forest structures. Thin Solid Films. 2020;709:138194. doi: 10.1016/j.tsf.2020.138194.
[42] Carini M, Shi L, Chamberlain TW, Liu M, Valenti G, Melle-Franco M, et al. Wall- and hybridisation-selective synthesis of nitrogen-doped double-walled carbon nanotubes. Angew Chem Int Ed Engl. 2019;58(30):10276–80. doi: 10.1002/anie.201905559.
[43] Zhu S, Dong X, Huang H, Qi M. Rich nitrogen-doped carbon on carbon nanotubes for high-performance sodium-ion supercapacitors. J Power Sources. 2020;459:228104. doi: 10.1016/j.jpowsour.2020.228104.
[44] Ye D, Su JT, Jiang Y, Yin ZP, Huang YA. Plasma-jet-induced programmable wettability on stretchable carbon nanotube films. Mater Today Phys. 2020;14:100227. doi: 10.1016/j.mtphys.2020.100227.
[45] Sui C, Pan Z, Headrick RJ, Yang Y, Wang C, Yuan J, et al. Aligned-SWCNT film laminated nanocomposites: role of the film on mechanical and electrical properties. Carbon. 2018;139:680–7. doi: 10.1016/j.carbon.2018.07.025.
[46] Varga M, Izak T, Vretenar V, Kozak H, Holovsky J, Artemenko A, et al. Diamond/carbon nanotube composites: Raman, FTIR and XPS spectroscopic studies. Carbon. 2017;111:54–61. doi: 10.1016/j.carbon.2016.09.064.
[47] Asim S, Javed MS, Hussain S, Rana M, Iram F, Lv D, et al. RuO_2 nanorods decorated CNTs grown carbon cloth as a free standing electrode for supercapacitor and lithium ion batteries. Electrochim Acta. 2019;326:135009. doi: 10.1016/j.electacta.2019.135009.
[48] Huo B, Jiang D, Cao X, Liang H, Liu Z, Li C, et al. N-doped graphene/carbon hybrid aerogels for efficient solar steam generation. Carbon. 2019;142:13–9. doi: 10.1016/j.carbon.2018.10.008.
[49] Luo X, Ma K, Jiao T, Xing R, Zhang L, Zhou J, et al. Graphene oxide-polymer composite langmuir films constructed by interfacial thiol-ene photopolymerization. Nanoscale Res Lett. 2017;12(1):12–99. doi: 10.1186/s11671-017-1864-8.
[50] Thomas HR, Marsden AJ, Walker M, Wilson NR, Rourke JP. Sulfur-functionalized graphene oxide by epoxide ring-opening. Angew Chem. 2014;53(29):7613–8. doi: 10.1002/anie.201404002.
[51] Wu K, Niu Y, Zhang Y, Yong Z, Li Q. Continuous growth of carbon nanotube films: From controllable synthesis to real applications. Compos Part A Appl Sci Manufact. 2021;144:106359. doi: 10.1016/j.compositesa.2021.106359.
[52] Nishizaka H, Kimura T, Sato Y, Yamamoto M, Nishida T, Motomiya K, et al. Slippage-inhibiting effect of interfacial

cross-linking of nanotubes by defluorination on the mechanical properties of free-standing multi-walled carbon nanotube yarns: Comparison with individual multi-walled carbon nanotubes. Carbon. 2021;179:1–12. doi: 10.1016/j.carbon.2021.03.066.

[53] Zou R, Liu F, Hu N, Ning H, Gong Y, Wang S, et al. Graphene/graphitized polydopamine/carbon nanotube all-carbon ternary composite films with improved mechanical properties and through-plane thermal conductivity. ACS Appl Mater Interfaces. 2020;12(51):57391–400. doi: 10.1021/acsami.0c18373.

[54] Jiang Q, Zhang Q, Wu X, Wu L, Lin JH. Exploring the interfacial phase and π–π stacking in aligned carbon nanotube/polyimide nanocomposites. Nanomaterials. 2020;10(6):1158. doi: 10.3390/nano10061158.

[55] Tian W, Li H, Qin B, Xu Y, Hao Y, Li Y, et al. Tuning the wettability of carbon nanotube arrays for efficient bifunctional catalysts and Zn–air batteries. J Mater Chem A. 2017;5(15):7103–10. doi: 10.1039/c6ta10505j.

[56] Duan Q, Wang S, Wang Q, Li T, Chen S, Zhang D, et al. Simultaneous improvement on strength, modulus, and elongation of carbon nanotube films functionalized by hyperbranched polymers. ACS Appl Mater Interfaces. 2019;11(39):36278–85. doi: 10.1021/acsami.9b12368.

[57] Xu Z, Liang Y, Ma X, Chen S, Yu C, Wang Y, et al. Recyclable thermoset hyperbranched polymers containing reversible hexahydro-s-triazine. Nat Sustain. 2020;3(1):29–34. doi: 10.1038/s41893-019-0444-6.

[58] Yu X, Liu D, Kang L, Yang Y, Zhang X, Lv Q, et al. Recycling strategy for fabricating low-cost and high-performance carbon nanotube TFT devices. ACS Appl Mater Interfaces. 2017;9(18):15719–26. doi: 10.1021/acsami.7b02964.